Dynamics of Core Electron Temperature Fluctuations during Sawtooth Oscillations on TEXT-U

Christopher Watts and R. F. Gandy
Department of Physics, Auburn University, Auburn, Alabama 36849
(Received 1 May 1995)

Core electron temperature fluctuations are measured in a tokamak plasma where some degree of time resolution is achieved. There is a strong correlation between the turbulence level and the phase of the sawtooth oscillations. The enhancement in fluctuations at the sawtooth crash is correlated to a steepening of the electron temperature gradient created as the sawtooth heat pulse propagates outward. A global linear relationship between the temperature fluctuation amplitude and the electron temperature gradient scale length is found.

PACS numbers: 52.25.Fi, 52.25.Gj, 52.55.Fa, 52.70.Gw

Toroidal magnetic confinement schemes still suffer from anomalously poor electron confinement and, as yet, the mechanism causing this transport is poorly understood. The term *anomalous transport* refers to the fact that random walk theories of confinement that include toroidal effects (neoclassical theories) underestimate electron transport by over an order of magnitude. Turbulent electrostatic fluctuations are considered by many as one likely candidate responsible for this transport [1–4]. The fluctuation-induced transport consists of two components, a particle flux Γ_e and a heat flux Q_e, given by

$$\Gamma_e = \langle \tilde{n}_e \tilde{v}_e \rangle = \langle \tilde{n}_e \tilde{E}_\theta \rangle / B , \quad (1)$$

$$Q_e = \tfrac{3}{2} \langle \tilde{p}_e \tilde{v}_e \rangle = \tfrac{3}{2} n_e \langle \tilde{T}_e \tilde{E}_\theta \rangle / B + \tfrac{3}{2} T_e \Gamma_e . \quad (2)$$

Here, $\tilde{n}_e$, $\tilde{T}_e$, and $\tilde{p}_e$ represent the fluctuations in electron density, temperature, and pressure, and $\tilde{v}_e \approx \tilde{E}_\theta / B = -\nabla_\theta \tilde{\varphi} / B$ is the radial component of the fluctuating $\mathbf{E} \times \mathbf{B}$ velocity. Thus the particle flux component results from the correlated fluctuations of plasma electric field and electron density, while the conducted heat flux is due to correlated fluctuations of the electric field and electron temperature.

Very recently, electron temperature fluctuations $\tilde{T}_{e,\mathrm{rms}}/T_e$ have been measured in both stellarator [5] and tokamak [6–8] plasmas using a technique correlating the plasma electron cyclotron emission (ECE). On TEXT-U, correlation radiometry of ECE (CRECE) correlates the emission of two largely overlapping sample volumes in two disjoint frequency bands [6–8]. This reduces the random, uncorrelated inherent wave noise of the ECE signal, while retaining the common temperature fluctuation amplitude. Detailed power spectra of these temperature fluctuations have been obtained over the low field side of the plasma in the equatorial plane [6]. The method has the advantage that the radiometer need not be absolutely calibrated. However, in order to reduce the wave noise to an acceptable level long time averaging is necessary, on the order of 1 s, and any temporal information of the turbulent fluctuations is lost.

In this Letter we report results in which some temporal information has been distilled. The quasiperiodic nature of tokamak sawtooth oscillations allows one to perform the correlation analysis synchronously with these oscillations, and thereby obtain spectra representing the evolution of the temperature fluctuations during the course of an average sawtooth period. [Sawteeth are characterized by a sudden drop ($\sim 5\% - 10\%$) in the electron temperature of the plasma core, followed by a rise in temperature outside the sawtooth inversion radius.] This provides some understanding of the time evolution of the temperature fluctuations, and perhaps insight into the mechanism of electrostatic turbulence and associated transport. The tacit assumption is that the dynamics of the turbulence are reproducibly linked to the sawtooth oscillations, a hypothesis verified *a posteriori*.

Measurements reported here have been made as outlined in [6] for circular plasmas ($R = 105$ cm, $a = 27$ cm) with $B_\phi \simeq 2$ T, $I_p = 200$ kA, and $\bar{n}_e = 2 \times 10^{13}$ cm^{-3}. Measurements are made in the equatorial plane from the low field side. The sample volume is a disk approximately 2 cm in diameter and 0.8 cm thick in the radial direction, allowing detection of wave numbers $k_\theta \lesssim 2$ cm^{-1} and $k_r \lesssim 5$ cm^{-1}.

To obtain the evolution of the temperature fluctuations during a sawtooth oscillation, ECE data are subdivided into eight bins representing different phases of the oscillation. All phases are relative to the *local* discontinuous change in electron temperature (sawtooth crash or rise) at the measurement location. The data in each phase bin are Fourier analyzed with a frequency resolution of $\frac{1}{32}$ of the Nyquist frequency to produce the time-averaged power spectrum for each sawtooth phase. Successive sawteeth are treated similarly, and the spectra of each sawtooth phase are ensemble averaged over many sawteeth to obtain the requisite statistics; each spectrum incorporates about 1000 sawteeth representing a 200 ms time average, where a typical sawtooth oscillation has a period of about 1.5 ms. However, because sawteeth periods are irregular, the number of points in each phase bin will vary. In addition, there is some ambiguity in determining the exact time of the sawtooth crash; the error is about ± 50 μs. For all data presented below, the quoted uncertainty in the temperature fluctuation amplitude is derived based on the statistical nature of the analysis procedure of randomlike

0031-9007/95/75(9)/1759(4)$06.00

data [9]. Thus $\varepsilon(\tilde{T}_{e,\mathrm{rms}}) \propto 1/\sqrt{N}$, where N is the number of independent samples. This statistical uncertainty dominates all systematic sources of error [6], which are small for results reported here.

We investigate the correlation between the fluctuation amplitude and changes in the electron temperature profile. Profiles at each phase of the sawtooth oscillation were reconstructed from eight fixed ECE channels by sweeping the plasma horizontally ± 1.5 cm during a single TEXT-U discharge [10]. There are two prominent regions: a flat region of the profile in the core and a gradient region outside which extends to the edge. The sawtooth inversion radius, located at $r/a \approx 0.3$ for these discharges, is located approximately at the boundary between the two regions.

Figure 1 depicts the evolution of the temperature fluctuation spectrum at $r/a = 0.13$, which is well inside the sawtooth inversion radius. Plotted is the normalized fluctuation power for each of the eight phases of a sawtooth oscillation (black line) along with the sawtooth averaged spectrum (gray), which is the same in each plot. The phases are labeled A–H, with A occurring at the sawtooth crash; the convention is sketched in the inset figure of plot A. Because of the relatively small signal, phases C through G have been ensemble averaged in order to obtain reasonable statistics. The dashed horizontal line represents the limit of statistical significance; points above this level are significant with regard to the correlation technique used to extract the temperature fluctuation from the inherently noisy ECE signal (see [6]). The spectra are normalized to the average electron temperature level for that particular sawtooth phase. Hence changes in the spectra represent only changes in the relative fluctuation level independent of any change in the bulk electron temperature.

As reported elsewhere [7], in the core ($r/a \approx 0$) before and during the sawtooth crash (phases H and A) there is an abrupt rise, on the order of a factor of 10, in the turbulence level at low frequency (<50 kHz). Ambiguity in determining the exact crash time distributes the power between the two phase bins that straddle the crash, A and H. Analysis of soft x-ray data and numerical and analytical models indicates that this increase is attributable to the Fourier components of the sudden drop in signal at the sawtooth crash (the power spectrum of the sawtoothing signal). After the crash, no significant turbulence is seen above the statistical limit except at very low frequencies (<25 kHz). Figure 2 clarifies the trend by plotting the electron temperature fluctuation amplitude $\tilde{T}_{e,\mathrm{rms}}/\overline{T}_e$ integrated over frequencies above 25 kHz, where the lower-frequency limit is chosen to eliminate low-frequency MHD oscillations. The variation between sawtooth crashes (B–G) is not significant.

Figure 3 shows the evolution at $r/a = 0.54$ outside the sawtooth inversion radius. Looking first at the sawtooth-averaged spectrum (gray line), immediately apparent is the appearance of a second "feature" in the spectrum which peaks at about 150 kHz. This "bump" is localized to the gradient region of the temperature profile and is distinguishable at all radii outside the inversion radius [6,7]. The implication is that the gradient, which is widely theorized to be the energy source of electron turbulence [1,2,11], is indeed the source of the turbulent fluctuations in the bump region. The center of the bump moves to a lower frequency as one moves radially outward. Assuming a plasma $\mathbf{E} \times \mathbf{B}$ rotation velocity, as measured by the heavy ion beam probe (HIBP) [12], the bump is consistent with a Doppler shifted turbulence feature rotating with the electron diamagnetic drift velocity $v_e^* = T_e/eB\alpha_n$, where α_n is the density gradient scale length. Density fluctuation diagnostics identify a similar feature in their spectra and find that this mode propagates in the electron diamagnetic drift direction [12,13].

As in the core, during the sawtooth rise the fluctuation level increases abruptly (phase A). This increase, however, is not confined exclusively to low frequency, but extends over the entire spectrum, and hence cannot be explained by the Fourier components of the sawtoothing

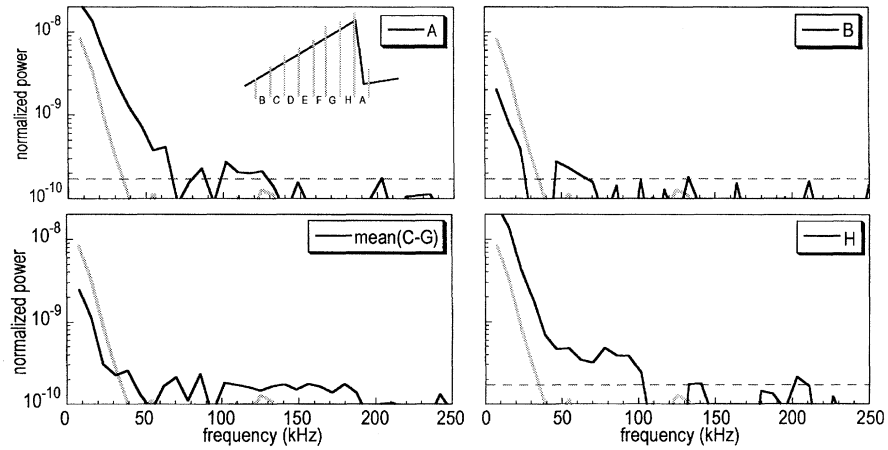

FIG. 1. Evolution of the electron temperature fluctuation power spectrum during a sawtooth oscillation at $r/a = 0.13$ (black). The gray line is the same spectrum averaged over sawteeth.

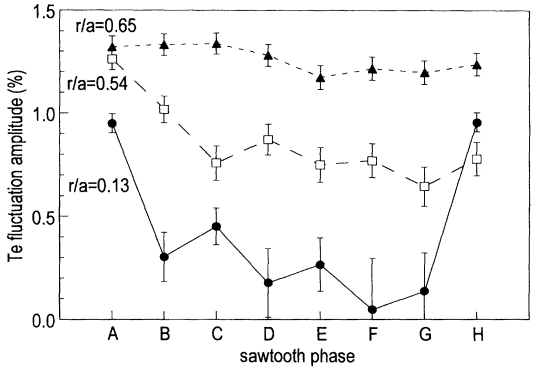

FIG. 2. Integrated electron temperature fluctuation amplitude for each of the sawtooth phases.

signal. Immediately after the rise the fluctuation power drops over the entire spectrum and continues to drop until about phase C (Fig. 2) when the turbulent energy seems to be largely dissipated. The fluctuations remain at this low level for the remainder of the sawtooth period. Again, the variation between sawteeth $(C-H)$ is probably not significant.

Figure 2 also shows data taken at $r/a = 0.65$. As before, there is an enhancement in the fluctuation power at the sawtooth rise which relaxes over the course of the sawtooth period. However, the effect is much less pronounced than at $r/a = 0.54$, while the enhancement lasts over several sawtooth phases $(A-D)$, before the drop in fluctuations $(D-E)$. This indicates that the energy source enhancing the turbulence is weaker, albeit more long lived. Further, only a fraction of the energy has dissipated by the final two phases. It appears that either the dissipation mechanism is not as efficient or the steady-state (between sawteeth) driving mechanism is stronger. Farther out in radius the effect of sawteeth on the spectra is minimal.

In order to understand the turbulence enhancement we look to the evolution of the electron temperature profile during a sawtooth oscillation. During a sawtooth crash, inside the inversion radius (the flat region) the entire profile rises and collapses simultaneously resulting in only a small change in the electron temperature gradient. Coincident with this is a rise only in the low-frequency ($\lesssim$70 kHz) turbulent temperature fluctuations, which is associated with the discontinuous nature of the crash. Outside the inversion radius, however, the propagating heat pulse leads to a significant steepening of the temperature gradient. One sees a commensurate enhancement of the temperature fluctuations in the bump region of the spectra. This increase in gradient is the likely source of the energy enhancing the turbulence in this region. At midradius the change in gradient is significant as the heat pulse propagates outward, and there is a large rise in the turbulent level. Farther out in radius the heat pulse is less potent and more long lived—the pulse shape more closely resembles a wave than a sawtooth—resulting in a smaller gradient change over a longer time period. This would account for the smaller increase in the turbulence level and a longer duration of the enhancement observed at larger radii.

Many electrostatic theories of transport predict that in the gradient region temperature fluctuations should scale as $\tilde{T}/T \propto 1/\langle k_\theta \rangle \alpha_T$, where $\langle k_\theta \rangle$ is the mean poloidal wave number and α_T is the temperature gradient scale length [1]. We are not as yet able to measure $\langle k_\theta \rangle$, which varies with several plasma parameters. Hence we look only for a functional dependence of $\tilde{T}_{e,\mathrm{rms}}/T_e$ with α_T. Plotted in Fig. 4 is the temperature fluctuation amplitude $\tilde{T}_{e,\mathrm{rms}}/T_e$ integrated over the bump region (75–225 kHz) versus the electron temperature gradient scale length $\alpha_T = |T_e/(dT_e/dr)|$ normalized to the plasma minor radius. Each of the eight symbols at each radius represents the eight phases of the sawtooth oscillation. The error in $\tilde{T}_{e,\mathrm{rms}}/T_e$, which again is derived from statistical considerations, is plotted for only some points. The error in α_T is 1 standard deviation in an ensemble of temperature profiles. Immediately apparent is the global linear relationship between turbulent fluctuation

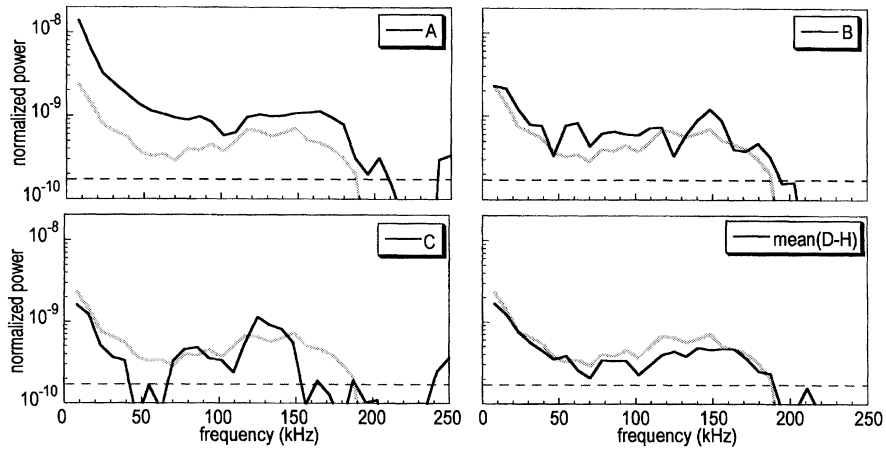

FIG. 3. Evolution of the electron temperature fluctuation power spectrum at $r/a = 0.54$.

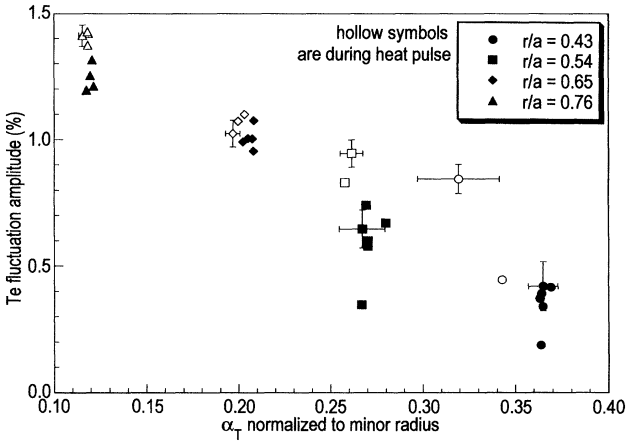

FIG. 4. Temperature fluctuation amplitude in the bump region versus temperature gradient scale length.

amplitude and α_T, which may account for the observation that the temperature fluctuations increase with increasing radius [6]. More significant, however, is that during the heat pulse phase (hollow symbols) α_T decreases while the fluctuations increase. Thus, as the sawtooth heat pulse propagates outward, there is a steepening of the temperature gradient and a commensurate rise in the temperature fluctuation amplitude. However, it is not clear that the change in fluctuation amplitude is consistent with the global linear relationship. The data indicate, rather, that the temperature fluctuations increase significantly for only modest changes in α_T. The global linear scaling of $\tilde{T}_{e,\mathrm{rms}}/T_e$ vs α_T appears to contradict marginal stability theories of anomalous transport, which argue that small changes in the temperature profile should result in a tremendous increase in fluctuation amplitude to restabilize the profile [1]. However, data during the sawtooth heat pulse appear to be consistent with marginal stability theories, since the temperature fluctuations rise significantly for modest changes in the local temperature gradient. More detailed profiles of both the temperature fluctuations and the temperature gradient scale length, as well as measurements of $\langle k_\theta \rangle$, are needed before a definitive conclusion is possible.

The significance of these results with regard to electrostatic transport has yet to be determined. Data are not yet available from the HIBP to ascertain whether a similar evolution of plasma potential fluctuations occurs. Further, since the wave number spectrum of these temperature fluctuations is difficult to measure, the relevance of the fluctuations in Eq. (2) is uncertain. In the edge a similar correlation between sawtooth oscillations and turbulent fluctuations has been identified, the sawtooth crash resulting in a significant increase in the associated transport [14]. Transport studies of sawtooth-free discharges in other machines are ambiguous [15,16].

In summary, by using the quasiperiodic nature of tokamak sawtooth oscillations we have obtained some temporal resolution of the turbulent electron temperature fluctuations. There is a strong correlation between $\tilde{T}_{e,\mathrm{rms}}/T_e$ and the phase of the sawtooth oscillation: The fluctuations increase during the crash/rise phase of the sawtooth. We find a global linear relationship between $\tilde{T}_{e,\mathrm{rms}}/T_e$ over the bump region of the power spectrum and the electron temperature gradient scale length and associate the rise in the fluctuation power during the sawtooth with a steepening of the electron temperature gradient. However, the enhancement of the temperature fluctuations during the sawtooth rise is greater than the linear scaling law predicts for changes in the local gradient scale length. Further study is needed to assess the relevance of these findings to anomalous transport.

We would like to thank David E. Newman, Pepi Cima, Alan Wootton, and Ken Gentle for their significant contribution. This work is supported by the United States Department of Energy under Grants No. DE-FG05-90ER54085-95 and No. DE-FG03-94ER-54241.

[1] P. C. Liewer, Nucl. Fusion **25**, 543 (1985).
[2] F. Wagner and U. Stroth, Plasma Phys. Controlled Fusion **35**, 1321 (1993).
[3] J. Sheffield, Rev. Mod. Phys. **66**, 1015 (1994).
[4] D. E. Newman, P. W. Terry, P. H. Diamond, Y. Liang, G. G. Craddock, A. E. Koniges, and J. A. Crotinger, Phys. Plasmas **1**, 1592 (1994).
[5] S. Sattler, H. J. Hartfuss, and W.-A. Team, Phys. Rev. Lett. **72**, 653 (1994).
[6] G. Cima, T. D. Rempel, R. V. Bravenec, R. F. Gandy, M. Kwon, C. Watts, and A. J. Wootton, Phys. Plasmas **2**, 720 (1995).
[7] C. Watts, G. Cima, R. F. Gandy, and T. D. Rempel, Rev. Sci. Instrum. **66**, 451 (1995).
[8] G. Cima and C. Watts, Rev. Sci. Instrum. **66**, 798 (1995).
[9] J. S. Bendat and A. G. Piersol, *Random Data: Analysis and Measurement Procedures* (John Wiley and Sons, New York, 1986).
[10] A Quick Time movie of the profile evolution is available from the gopher server hagar.ph.utexas.edu in the directory TEXT-U Tokamak Information/TEXT-U Data and Experiments/ECE Quick Time Movie.
[11] D. E. Newman, P. W. Terry, and P. H. Diamond, Phys. Fluids B **4**, 599 (1992).
[12] A. Fujisawa, A. Ouroua, J. W. Heard, T. P. Crowley, P. M. Schoch, K. A. Conner, R. L. Hickok, and A. J. Wootton (to be published).
[13] Y. Karzhavin (private communication).
[14] T. L. Rhodes, C. P. Ritz, and H. Lin, Phys. Rev. Lett. **65**, 583 (1990).
[15] V. P. Bhatnagar, D. Campbell, J. P. Christiansen, J. G. Cordey, J. Jacquinot, D. F. H. Start, P. Thomas, and K. Thomsen, in *Proceedings from the 15th European Conference on Controlled Fusion and Plasma Heating* edited by S. Pesic and J. Jacquinots (European Physical Society, Geneva, 1988), Vo. 12, Part I, p. 358.
[16] U. Stroth, G. Fussmann, K. Krieger, V. Mertens, F. Wagner, M. Bessenrodt-Weberpals, R. Büchse, L. Giannone, W. Herrmann, E. Simmet, K. Steuer, and ASDEX Team, Nucl. Fusion **31**, 2291 (1991).